Supplementary Figure S1. HSET RNAi does not significantly affect spindle bipolarity. (A) Western blot of cells treated with either control or HSET RNAi and then probed with anti-HSET and anti-tubulin antibodies. (B) Immunofluorescence with anti-HSET antibodies in control and HSET RNAi cells. The remaining spindle pole staining after HSET knockdown is due to non-specific staining of another protein. Scale bar, 10 μm. (C) Quantification of the percentage of monopolar, bipolar, and multi-polar spindles after HSET RNAi in which a total of 300 cells were scored in three independent experiments. The mean ± SEM is shown.

Supplementary Figure S2. Perturbation of HSET affects spindle length. (A) HeLa cells transfected with control or HSET siRNAs or stably overexpressing GFP-HSET were treated with ice cold media for 10 min to depolymerize cold-labile MTs. Cells were subsequently processed for immunofluorescence to visualize MTs (magenta), HSET or GFP-HSET (green), and DNA (blue). Scale bar, 10 μm. (B) Quantification of the length distribution of the bulk MTs under each experimental condition with the superimposed best fit Gaussian distribution. A total of 60 structures were measured in three independent experiments. Average MT lengths: control, 8.3 ± 0.6 μm; HSET RNAi, 6.7 ± 0.8 μm; and HSET overexpression, 9.6 ± 0.5 μm.

Supplementary Figure S3. The N593K mutation uncouples MT binding and MT stimulated ATPase activity in HSET. (A) GFP-HSET or GFP-HSET N593K proteins (250 nM) were assayed for steady-state ATPase activity in the presence of increasing amounts of MTs (0-3 μM). The data were fit to Equation 1: Rate = k_{cat} * MT_t /(K_m + MT_t). (B) Summary table of

the kinetic values derived from (A). (C) GFP-HSET or GFP-HSET N593K (0.35 μM) were incubated with increasing concentrations of pre-assembled MTs (0- 0.7 μM) for 15 min at RT. MT-bound proteins were separated from soluble proteins by ultracentrifugation, and equivalent amounts of supernatant (S) and pellet (P) fractions were analyzed by SDS-PAGE and Coomassie Blue staining. (D) The binding curves were fit to Equation 2 $MT \cdot E = E_0 + (a/3) - (2/3)(a^2 - 3b)^{1/2}\cos(Z/3)$ and represent the average of four experiments for GFP-HSET and six experiments for the GFP-HSET N593K mutant. (E) Summary table of binding data from (D).

Supplementary Figure S4. HSET N593K does not stimulate spindle assembly in extracts. GFP (A), GFP-XCTK2 (B), GFP-HSET (C), or GFP-HSET-N593K (D) were added to CSF extracts at a 2.5-fold molar excess relative to endogenous XCTK2 and incubated for 30 min to allow for spindle assembly. Each panel represents a montage of images in which the MTs are magenta and the DNA is blue. Scale bar, 10 μm. (E) Western blot of the samples from each reaction in A-D to show equal amount of proteins were added into the extract. (F) Quantification of the average percentage of structures with the indicated morphologies from four independent extracts in which at least 100 structures were scored per experiment. The mean ± SEM is reported.

Supplementary Figure S5. XCTK2 functions during spindle maintenance and affects spindle morphology. GFP, GFP-XCTK2, GFP-XCTK2 NLSa, and GFP-XCTK2 NLSb proteins were added to preformed spindles from egg extracts at a 5-fold molar excess relative

to endogenous XCTK2. Representative fields of view showing MTs (magenta), the GFP fusion protein (green) and DNA (blue). Scale bar, 50 μm.

Fig. S1

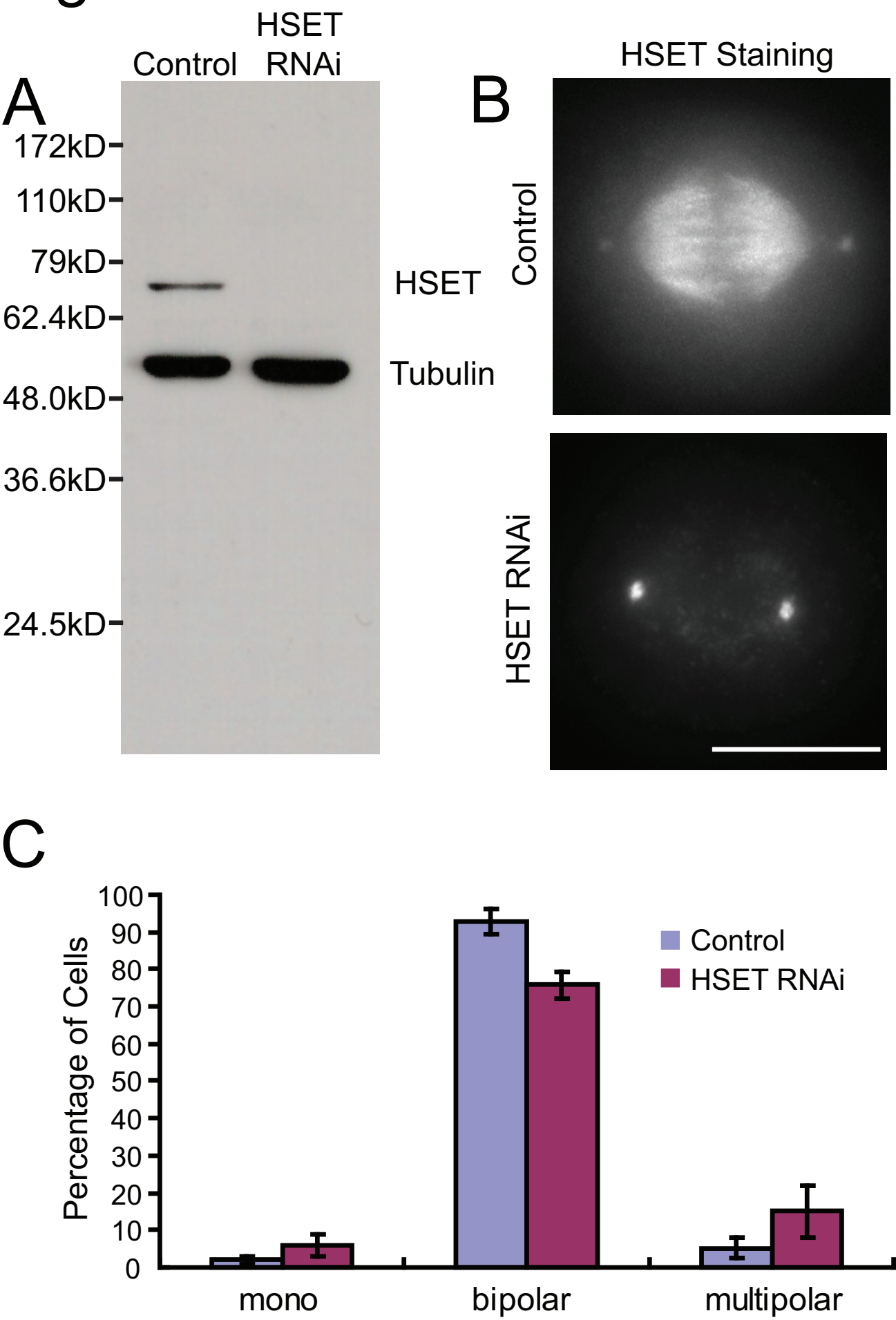
A
Control
HSET RNAi
172kD
110kD
79kD
62.4kD
48.0kD
36.6kD
24.5kD
HSET
Tubulin
B
HSET Staining
Control
HSET RNAi
C
Percentage of Cells
100
90
80
70
60
50
40
30
20
10
0
Control
HSET RNAi
mono
bipolar
multipolar

Fig. S2

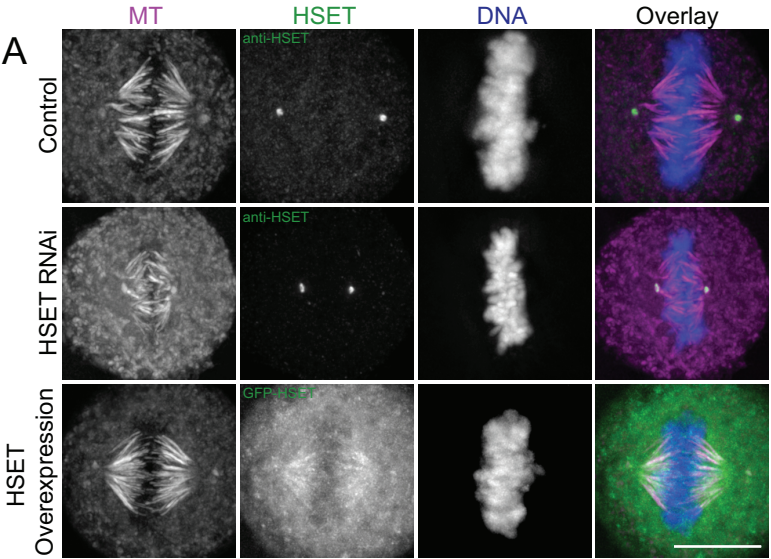
MT
HSET
DNA
Overlay
A
Control
HSET RNAi
HSET Overexpression
anti-HSET
anti-HSET
GFP-HSET

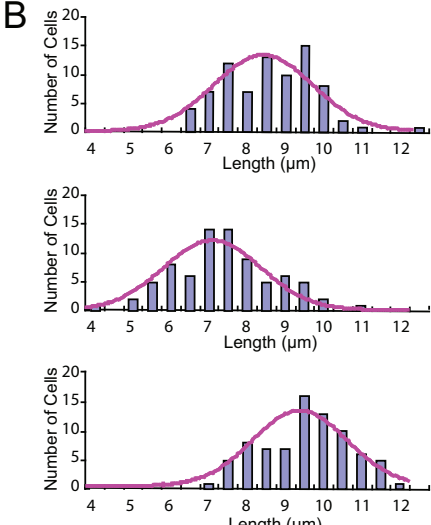
B
Number of Cells
Length (μm)
Number of Cells
Length (μm)
Number of Cells
Length (μm)

Fig. S3

A

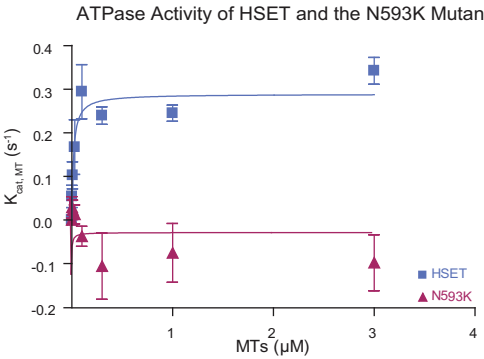

B

ATPase Activity of HSET and the N593K Mutant

	HSET	N593K
$K_{cat, MT}$	0.29 s^{-1}	-0.029 s^{-1}
95% Confidence Interval	0.24 to 0.34 s^{-1}	-0.006 to -0.001 s^{-1}

C

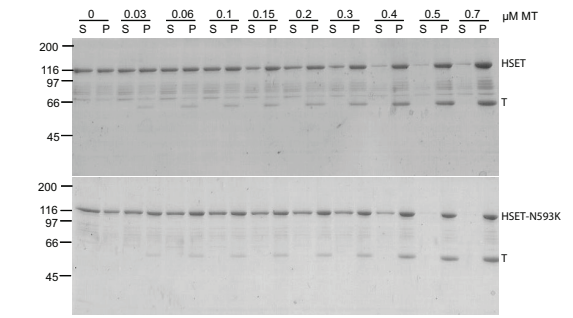

D

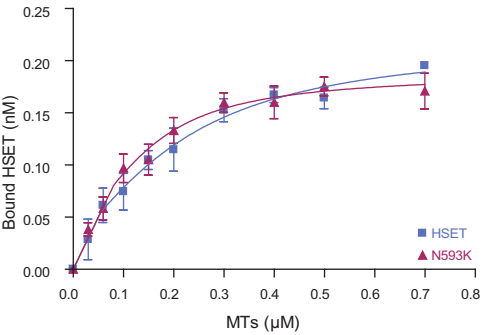

E

MT Binding Affinity of HSET and the N593K Mutant

	HSET	N593K
K_{d1}	1 x 10^{-7} μM	1 x 10^{-7} μM
95% Confidence Interval	0 to 0.0052 μM	0 to 0.0065 μM
K_{d2}	0.13 μM	0.072 μM
95% Confidence Interval	0 to 0.43 μM	0 to 0.24 μM

Fig. S4

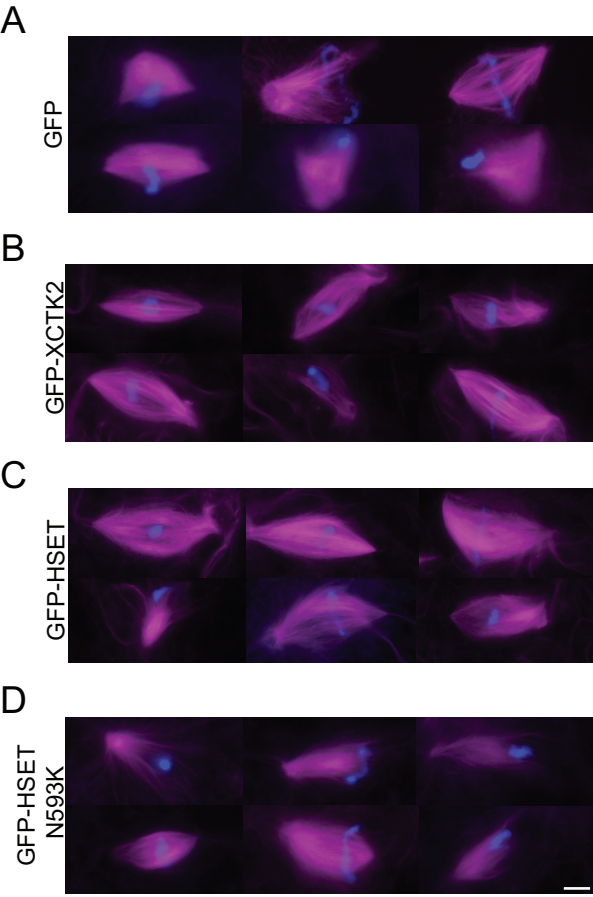
A
GFP
B
GFP-XCTK2
C
GFP-HSET
D
GFP-HSET
N593K

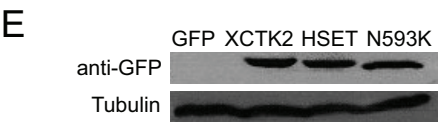
E
GFP XCTK2 HSET N593K
anti-GFP
Tubulin

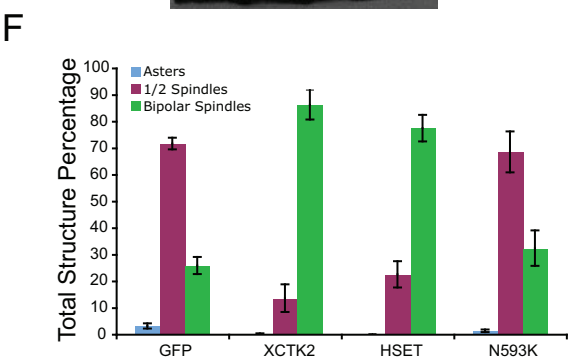
F
Total Structure Percentage
100
90
80
70
60
50
40
30
20
10
0
Asters
1/2 Spindles
Bipolar Spindles
GFP
XCTK2
HSET
N593K

Fig. S5

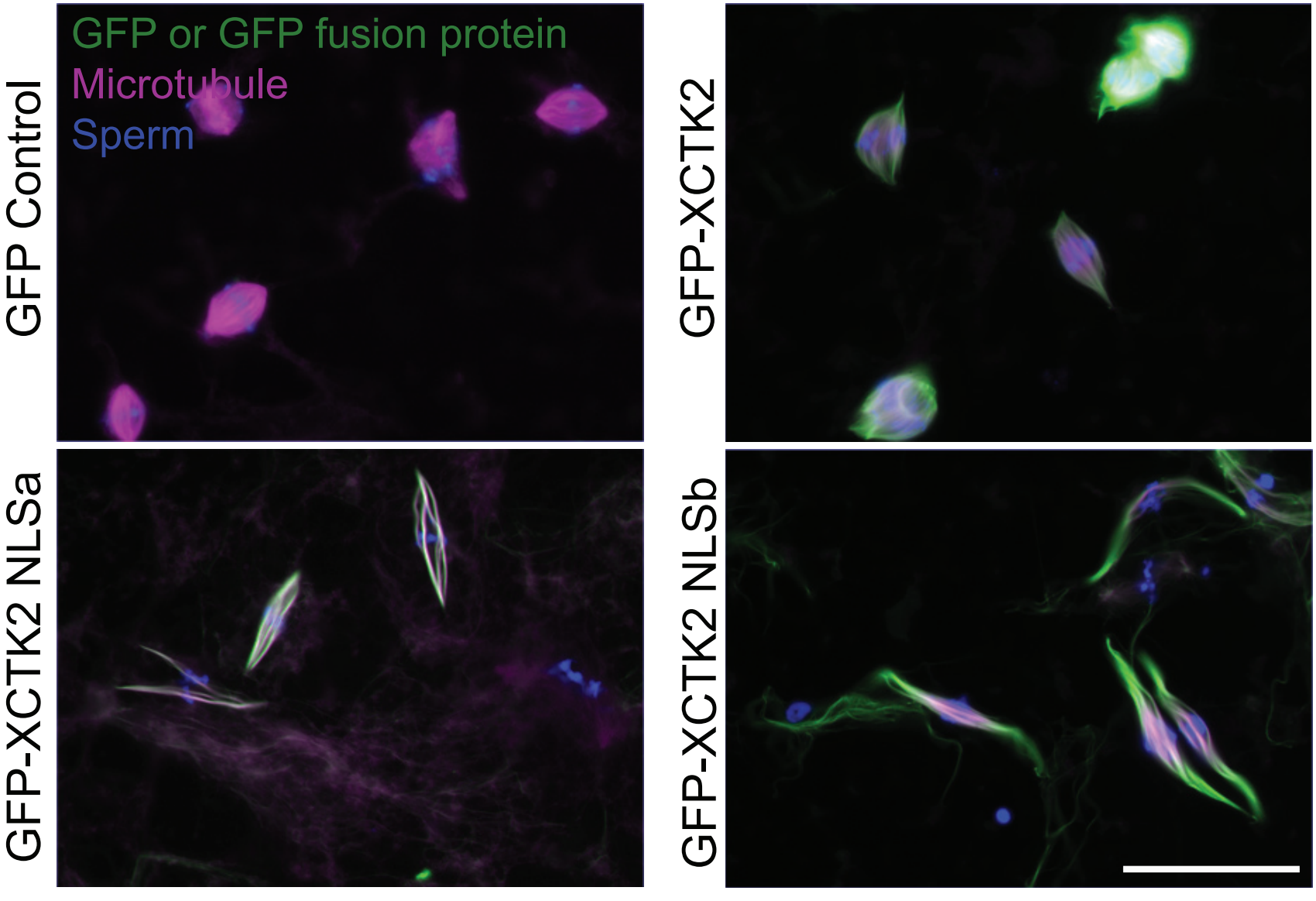
GFP or GFP fusion protein
Microtubule
Sperm
GFP Control
GFP-XCTK2
GFP-XCTK2 NLSa
GFP-XCTK2 NLSb